Journal of Alloys and Compounds 509 (2011) 977–981

Contents lists available at ScienceDirect

Journal of Alloys and Compounds

journal homepage: www.elsevier.com/locate/jallcom

High-temperature thermoelectric properties of late rare earth-doped $Ca_3Co_4O_{9+\delta}$

N.V. Nong[a], Chia-Jyi Liu[a,*], M. Ohtaki[b]

[a] Department of Physics, National Changhua University of Education, No. 1 Jin De Road, Changhua City, 500 Taiwan, ROC
[b] Interdisciplinary Graduate School of Engineering Sciences, Kyushu University, Fukuoka, 816-8580, Japan

ARTICLE INFO

Article history:
Received 23 May 2010
Received in revised form
23 September 2010
Accepted 24 September 2010

Keywords:
Thermoelectric materials
Oxide materials
Solid state reactions
Thermoelectrics

ABSTRACT

Misfit-layered oxides $Ca_{3-x}Ln_xCo_4O_{9+\delta}$ with Ln = Dy, Er, Ho, and Lu were synthesized using solid state reactions. The resulting samples were hot-pressed (HP) at 1123 K in air for 2 h under a uniaxial pressure of 60 MPa. Thermoelectric properties of $Ca_{3-x}Ln_xCo_4O_{9+\delta}$ were investigated up to 1200 K. Both the Seebeck coefficient and electrical resistivity increase upon Ln substitution for Ca. Among the Ln-doped samples, the magnitude of Seebeck coefficient tends to increase with decreasing ionic radius of Ln^{3+}. The Ln-doped samples exhibit a lower thermal conductivity than the non-doped one due to a decrease of their lattice thermal conductivity. The dimensionless figure of merit, *ZT*, reaches 0.36 at 1073 K for the $Ca_{2.8}Lu_{0.2}Co_4O_{9+\delta}$ sample, which is about 1.6 times larger than that for the non-doped counterpart.

1. Introduction

A large amount of thermal energy from many industrial processes or similar sources is available as waste heat, which is difficult to reclaim due to the dispersed nature and relatively small scale. Thermoelectric (TE) generation can offer a very promising method to overcome these problems by converting the waste heat directly into electricity [1]. Good thermoelectric materials are required to have high dimensionless figure of merit $ZT = S^2\sigma T/\kappa$, where *S* is the Seebeck coefficient, σ the electrical conductivity, κ the thermal conductivity, and *T* the operating temperature. Besides, thermoelectric materials are required to be stable at high temperatures. Oxides are one of the best candidate materials for this requirement. In recent years, layered cobalt oxides have gained great attention since $NaCo_2O_4$ single crystal was found to exhibit good thermoelectric properties [2]. However, practical application for power generation using waste heat is quite limited due to the Na volatility and poor resistance to humidity for $NaCo_2O_4$. Another Co-based oxide $Ca_3Co_4O_{9+\delta}$ has been intensively investigated due to its thermal and chemical stabilities at high-temperature in air [3–9] along with good thermoelectric performance e.g., $ZT = 0.83$ at 973 K for the single crystal [3]. The composition of $Ca_3Co_4O_{9+\delta}$ is better expressed as $[Ca_2CoO_3][CoO_2]_{b_1/b_2}$ with the misfit-layered structure featuring different periodicities along the *b*-axis with b_1 referring to the *b*-axis length of NaCl-type $[Ca_2CoO_3]$ sublattice and b_2 referring to the *b*-axis length of $[CoO_2]$ sublattice. The crystal structure of $Ca_3Co_4O_{9+\delta}$ can be viewed as being comprised of two subsystems, i.e., the distorted NaCl-type $[Ca_2CoO_3]$ sublattice and the CdI_2-type $[CoO_2]$ sublattice alternatively stacking along the *c* axis [4]. For practical fabrication of TE devices, single crystalline samples are too small and expensive. It is more feasible to enhance the TE properties of polycrystalline materials. Many attempts have been made to optimize the thermoelectric performance of $Ca_3Co_4O_{9+\delta}$ by either partially substituting cations or using appropriate fabrication methods such as hot-pressing (HP) or spark plasma sintering (SPS) techniques. Partial replacement of cations in $Ca_3Co_4O_{9+\delta}$ have been carried out on either the Ca site [10–21] or the Co sites. [22–25] It has been reported that partial substitution for Ca by heavier ions with trivalence such as Eu^{3+} [10], Nd^{3+} [11], Bi^{3+} [12], Y^{3+} [14], Yb^{3+} [18] Gd^{3+} and Y^{3+} [19] is effective in improving thermoelectric properties, e.g., $ZT \approx 0.25$ for the Bi-doped and $ZT \approx 0.3$ for the Eu-doped samples at ca. 1000 K. Addition of Ag in $Ca_3Co_4O_{9+\delta}$ has been recently reported to enhance the thermoelectric power factor [13,17,21]. Notably, a *ZT* value of 0.5 at 1000 K is obtained for $Ca_{2.7}Ag_{0.3}Co_4O_9$/Ag–10 wt% composite [17].

In this paper, we report the preparation of various selected late rare earth doped samples $Ca_{3-x}Ln_xCo_4O_{9+\delta}$ (Ln = Er, Dy, Ho and Lu) using hot-pressing techniques and their high-temperature thermoelectric properties. We find that the Lu-doped sample has the largest power factor among $Ca_{2.9}Ln_{0.1}Co_4O_{9+\delta}$ (Ln = Er, Dy, Ho and Lu). In order to obtain better thermoelectric properties, we focus on investigating $Ca_{3-x}Lu_xCo_4O_{9+\delta}$ with $x = 0.1$, 0.2, and 0.3. As a result, we find that the magnitude of *ZT* for the $Ca_{2.8}Lu_{0.2}Co_4O_{9+\delta}$ sam-

* Corresponding author. Tel.: +886 4 7232105x3337; fax: +886 4 728 0698.
E-mail address: liucj@cc.ncue.edu.tw (C.-J. Liu).

0925-8388/$ – see front matter © 2010 Elsevier B.V. All rights reserved.
doi:10.1016/j.jallcom.2010.09.150

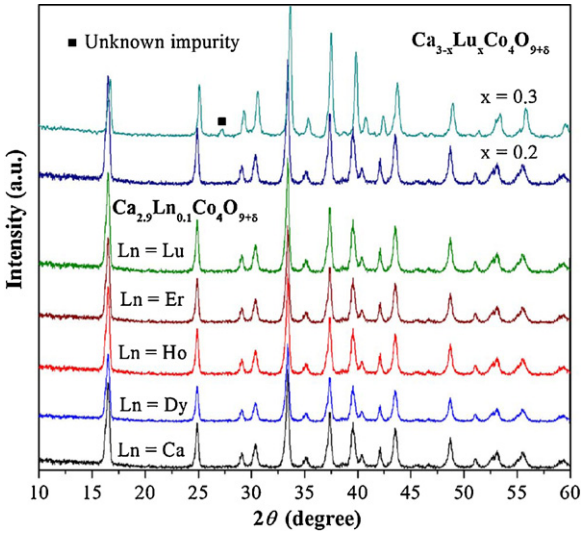

Fig. 1. Powder X-ray diffraction patterns for $Ca_{2.9}Ln_{0.1}Co_4O_{9+\delta}$ (Ln = Dy, Ho, Er and Lu) and $Ca_{3-x}Lu_xCo_4O_{9+\delta}$ with $x = 0.2$, and 0.3 samples.

ple attains 0.36 at 1073 K, which seems to be the most significant improvement as compared to Bi-, Sr-, Na-, Nd-, Gd-, Eu-, Y-, Gd/Y- and Yb-doped samples.

2. Experimental details

The polycrystalline $Ca_{3-x}Ln_xCo_4O_{9+\delta}$ samples with Ln = Dy, Er, Ho, and Lu were synthesized by solid state reactions from $CaCO_3$ (99.5%), Co_3O_4 (99.7%) and Ln_2O_3 (99.9%) powders for $x = 0$, 0.1, 0.2, and 0.3. The $CaCO_3$ and Ln_2O_3 powders were first mixed and milled for 1 h using a rocking mill, which is a milling system vibrating with two containers. The mixture was then taken out and milled with Co_3O_4 for another 1 h. The resulting powders were ball milled with ethanol for 24 h, followed by drying and calcination in air at 1173 K for 24 h. The calcined samples were pressed into pellets and sintered at 1223 K in flowing O_2 gas for 24 h to ensure the desired oxygen nonstoichiometry of $Ca_{3-x}Ln_xCo_4O_{9+\delta}$. The oxygen content $(9+\delta)$ was determined using iodometric titration [22]. The size of δ is about 0.33 for the non-doped sample and the difference is less than 1% among the Ln-doped samples. The pellets of the samples were re-ground and then hot-pressed (HP) at 1123 K in air for 2 h under a uniaxial pressure of 60 MPa. X-ray powder diffraction (XRD) analysis was carried out on a Rigaku RINT2002PC diffractometer with Cu K_α radiation. Thermogravimetric (TG) and differential thermal analyses (DTA) were carried out from room temperature to 1500 K. The relative densities of all the non-doped and Ln-doped samples were measured using Archimedes' method. The microstructure of the HP-samples was observed by scanning electron microscopy (SEM). The electrical resistivity and the Seebeck coefficient were measured simultaneously from room temperature to 1200 K in air using an Ozawa RZ2001i thermoelectric property measurement system. The thermal conductivity was determined from the thermal diffusivity and the specific heat capacity measured by laser flash technique from room temperature to 1073 K using LFA-502 laser flash system.

3. Results and discussion

Fig. 1 presents the powder X-ray diffraction (XRD) patterns of $Ca_{2.9}Ln_{0.1}Co_4O_{9+\delta}$ (Ln = Dy, Er, and Ho) and $Ca_{3-x}Lu_{0x}Co_4O_{9+\delta}$ $x = 0.1$, 0.2 and 0.3. For the samples with $x = 0.1$ and $x = 0.2$, all XRD peaks can be indexed as the $Ca_3Co_4O_{9+\delta}$ phase [4]. However, the Lu-doped sample with $x = 0.3$ exhibits an impurity peak at about 27°, which is similar to the case of Eu substitution [10]. Moreover, the XRD peak positions of this sample are slightly shifted, e.g., the peaks at 16°, 25° and 33.4°. The structure refinement using a *Jana2006* Rietveld program were carried out for the non-doped and selected Ln-doped samples with Ln = Ho and Lu. We find that the misfit ratio of b_1/b_2 and β slightly changed ($b_1/b_2 = 1.6132$, 1.6140 and 1.6133; $\beta = 98.054$, 98.087 and 98.1 for the non-doped, Ln = Ho and Ln = Lu samples, respectively). The TG and DTA analyses up to about 1500 K in air reveal that there is no significant change of weight from 300 K to 1200 K, indicating that the samples are thermally stable up to 1200 K. All the hot-pressed non-doped and Ln-doped samples have

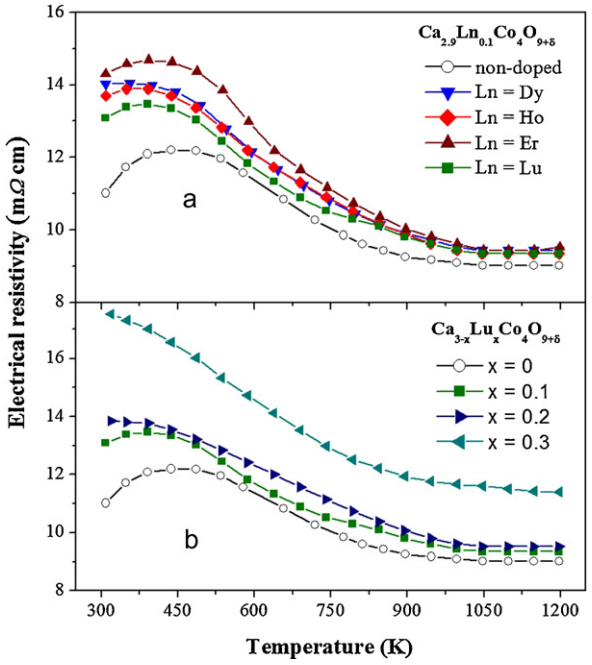

Fig. 2. Temperature dependence of the electrical resistivity: (a) is for non-doped and $Ca_{2.9}Ln_{0.1}Co_4O_{9+\delta}$ (Ln = Dy, Ho, Er and Lu) and (b) for $Ca_{3-x}Lu_xCo_4O_{9+\delta}$ with $x = 0$, 0.1, 0.2, and 0.3, respectively.

a high bulk density and the relative density is larger than 95% of the theoretical X-ray density 4.68 g/cm^3 [4]. The density of all doped samples for $x \geq 0.2$ are about 1% higher than the non-doped one except for the $x = 0.3$ samples.

Fig. 2a and b show the electrical resistivity (ρ) as a function of temperature for $Ca_{2.9}Ln_{0.1}Co_4O_{9+\delta}$ (Ln = Dy, Ho, Er and Lu) and $Ca_{3-x}Lu_xCo_4O_{9+\delta}$ with $x = 0$, 0.1, 0.2, and 0.3 samples, respectively. A broad hump can be readily seen in the ρ–T curve of these cobaltite samples, resembling the temperature dependence of the in-plane resistivity for a single crystal in the corresponding temperature regime. The hump maximum occurs around 450 K for the non-doped sample, that is, the ρ–T curve shows metal-like behavior below 450 K ($d\rho/dT < 0$), whereas it shows semiconductor-like behavior above 450 K ($d\rho/dT > 0$), which can also be described as a metal–nonmetal transition. The hump maximum seems to shift to a lower temperature as the Lu content increases (Fig. 2b). An incoherent metal with the quasiparticle resonance becoming strongly temperature dependent is used to explain the resistivity behavior in the temperature range between 142 K and 510 K for the non-doped sample. The metal-nonmetal transition could arise from the pseudogap due to the disappearance of quasiparticle resonance [7]. Partial substitution of Ln^{3+} for Ca^{2+} causes an increase of ρ and the effect is more substantial at $T < 600$ K. This might be ascribed to a decrease of Co^{4+} based on charge neutrality with the assumption of O^{2-}. The Co^{4+} ion is commonly considered as the hole carrier being responsible for the charge transport in both Na_xCoO_2 and $Ca_3Co_4O_{9+\delta}$ [26–28]. It should be noted that the temperature coefficient of resistivity becomes smaller at higher temperatures. Among the Ln-doped samples at a given temperature, the magnitude of resistivity tends to increase roughly with decreasing ionic radius of Ln^{3+} except the case of Ln = Er.

Fig. 3 shows SEM images from fractured surfaces of the non-doped sample, $Ca_{2.9}Er_{0.1}Co_4O_{9+\delta}$, and $Ca_{3-x}Lu_xCo_4O_{9+\delta}$ with $x = 0.1$ and 0.2. It can be seen from Fig. 3 that the plate-like grains are more pronounced for the non-doped sample, while they become thinner and smaller after partial substitution of Er or Lu. Among the investigated Ln-doped samples, microstructure of the Er-doped

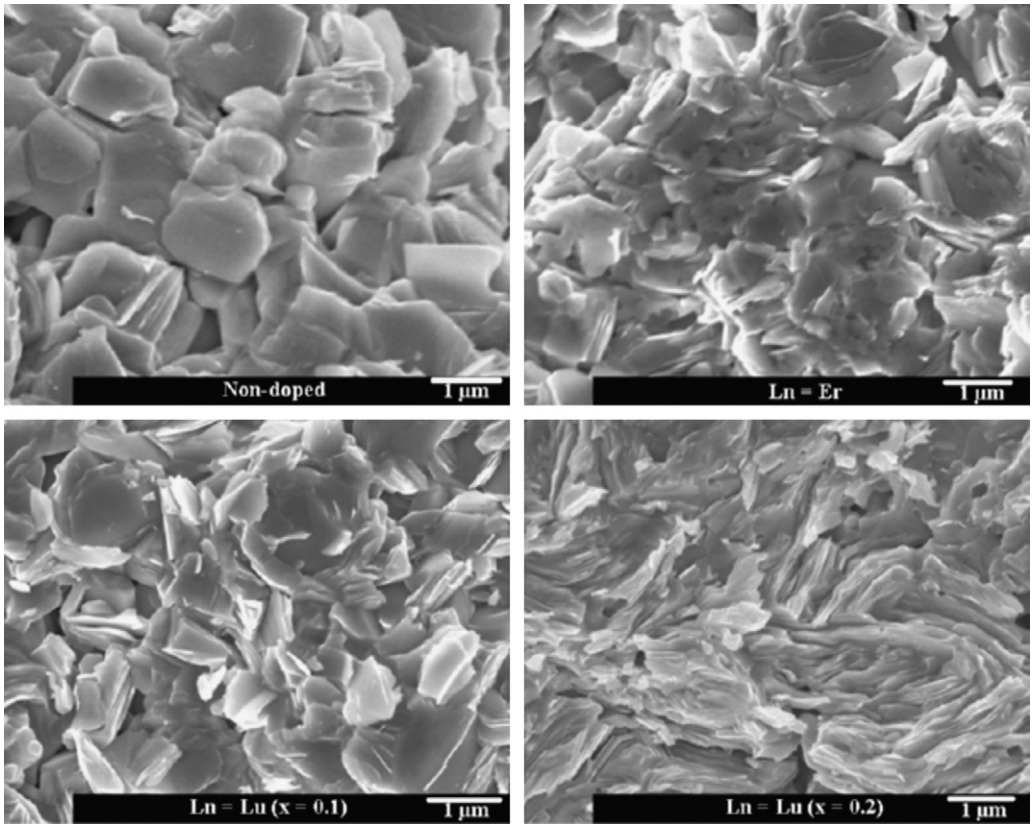

Fig. 3. SEM images from fractured surfaces of the samples for non-doped, $Ca_{2.9}Ln_{0.1}Co_4O_{9+\delta}$ (Ln = Er and Lu) and $Ca_{3-x}Lu_xCo_4O_{9+\delta}$ with $x = 0.2$.

sample is somewhat deteriorated, which might be associated with the most increase of the electrical resistivity.

Fig. 4 shows the temperature dependence of the Seebeck coefficient (S) for $Ca_{2.9}Ln_{0.1}Co_4O_{9+\delta}$ (Ln = Dy, Er, Ho, and Lu) and $Ca_{3-x}Lu_xCo_4O_{9+\delta}$ with $x = 0.2$, and 0.3 samples. For all the investigated samples, S shows positive values in the whole measured temperature region, indicating the p-type conduction; S increases with increasing temperature and levels off at 1050 K. It can be clearly seen that partial substitution of Ln for Ca results in an increase of S and its size increases with increasing Ln concentration. A possible scenario for these results is described as follows.

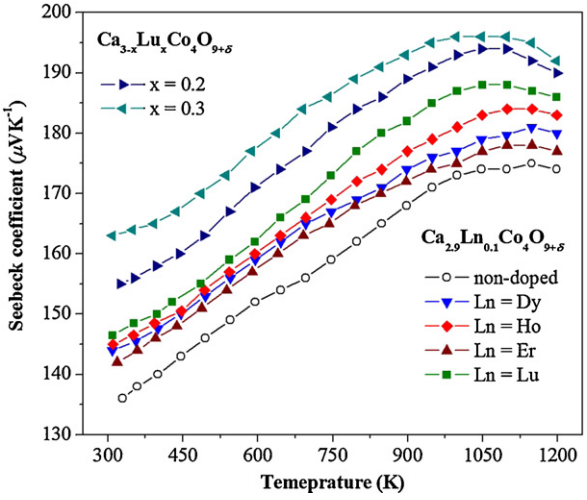

Fig. 4. Temperature dependence of the Seebeck coefficient for $Ca_{2.9}Ln_{0.1}Co_4O_{9+\delta}$ (Ln = Dy, Ho, Er and Lu) and $Ca_{3-x}Lu_xCo_4O_{9+\delta}$ with $x = 0.2$, and 0.3 samples.

High-temperature thermoelectric power can be estimated by using the modified Heikes formula [26].

$$S = -\frac{k_B}{e}\ln\left(\frac{g_3}{g_4}\frac{x}{1-x}\right) \quad (1)$$

where g_3, and g_4 are the number of configuration of the Co^{3+} and Co^{4+} ions, respectively; x is the fraction of the Co^{4+} on the Co sites. According to the X-ray absorption study of the $Ca_3Co_4O_{9+\delta}$, both Co^{3+} (t_{2g}^6) and Co^{4+} (t_{2g}^5) are found to be in the low spin state [5,10,14,23,29], yielding $g_3 = 1$ and $g_4 = 6$, respectively. From Eq. (1), one would expect that the magnitude of S increases with decreasing x. This means that lower concentration of Co^{4+} would lead to higher S. This is consistent with our findings: (1) trivalent Ln^{3+} substitution for divalent Ca^{2+} leads to an increase of S, which could be attributed to a decrease of Co^{4+} concentration; (2) Higher Lu^{3+} content (x) leads to a decrease of Co^{4+} concentration and thus an increase of S. Interestingly, it appears that the smallest ionic radius of Lu^{3+} in this series of Ln^{3+} has the smallest ρ and largest S.

Fig. 5 shows the calculated power factor (S^2/ρ) of $Ca_{2.9}Ln_{0.1}Co_4O_{9+\delta}$ (Ln = Dy, Er, Ho, and Lu) and $Ca_{3-x}Lu_xCo_4O_{9+\delta}$ with $x = 0.2$, and 0.3 samples. The power factor is enhanced by partial substitution of Ho^{3+} and Lu^{3+} for Ca^{2+}. In particular, the Lu-doped sample with $x = 0.2$ has the most improvement. Although the Lu-doped sample with $x = 0.3$ shows the highest S, the power factor is not much improved due to a large decrease of the electrical conductivity. The magnitude of the power factor is 0.336, 0.362, 0.379, and 0.398 mW m^{-1} K^{-2} for the samples of non-doped, Ho-, Lu-doped with $x = 0.1$ and Lu-doped with $x = 0.2$, respectively. The size of the Ln^{3+} on the electronic transport properties seems to arise from the internal chemical pressure imposing on the structure. The internal chemical pressure arises from substitution of different size of ions in the parent lattice. The internal chemical pressure could induce a change of the bandwidth. The bandwidth

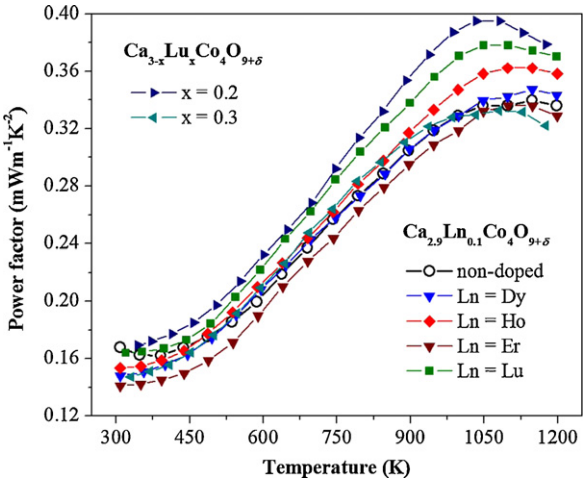

Fig. 5. Power factor as a function of temperature for $Ca_{2.9}Ln_{0.1}Co_4O_{9+\delta}$ (Ln = Dy, Ho, Er and Lu) and $Ca_{3-x}Lu_xCo_4O_{9+\delta}$ with $x = 0.2$, and 0.3 samples.

depends on the bond length and bond angle, which are responsible for the charge transport [30]. However, it would need further studies.

Fig. 6(a) shows the thermal conductivity (κ) as a function of temperature for the samples of non-doped, Ho-doped with $x = 0.1$ and Lu-doped with $x = 0.1$ and 0.2. Partial substitution of Ln^{3+} for Ca^{2+} causes a decrease of κ, which decreases with increasing lanthanide concentration. Total thermal conductivity (κ_{total}) can be expressed as $\kappa_{total} = \kappa_{ph} + \kappa_e$, where κ_{ph} and κ_e are the lattice and electronic contribution, respectively. For $Ca_3Co_4O_{9+\delta}$, the contribution of κ_e to κ_{total} is small (i.e., less than 0.1 W/m K^2) according to the Wiedemann–Franz law, which can be expressed as

$$\kappa_e = L\sigma T \quad (2)$$

where the proportionality constant L is the Lorenz number and σ is the electrical conductivity. The small κ_e indicates that the major contribution to κ_{total} arises from the phonon term κ_{ph}. Even though

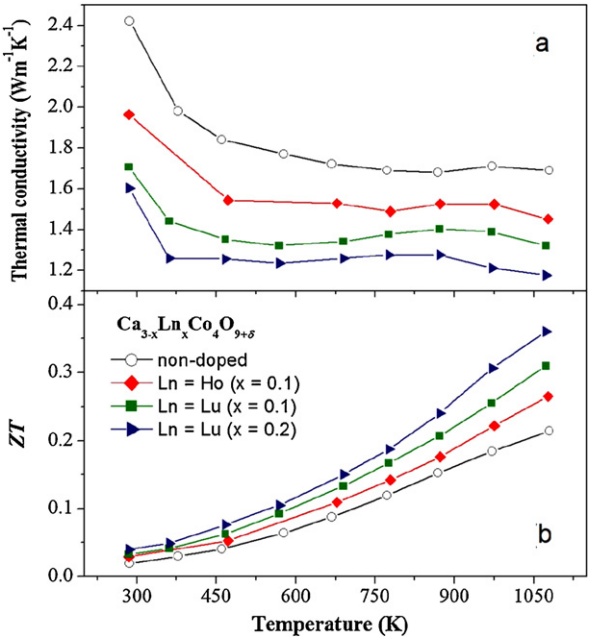

Fig. 6. Temperature dependence of the thermal conductivity (a) and dimensionless figure of merit, ZT (b) for non-doped, $Ca_{2.9}Ln_{0.1}Co_4O_{9+\delta}$ (Ln = Ho and Lu), and Lu-doped with $x = 0.2$ samples.

the decrease of electrical conductivity leads to a decrease of κ_e, which is caused by partial substitution of Ln^{3+} for Ca^{2+}, the decease of κ_{total} can be mainly attributed to the reduction of lattice contribution arising from incorporation of heavier Ln^{3+} ions in the structure as compared to Ca^{2+} ions. Fig. 6(b) illustrates the temperature dependence of dimensionless figure of merit ZT for the samples of non-doped, Ho-doped with $x = 0.1$ and Lu-doped with $x = 0.1$ and 0.2. The size of ZT of all samples tends to increase with increasing temperature and is significantly improved by the Ho and Lu substitution. The highest magnitude of ZT is about 0.36 at 1073 K for the Lu-doped with $x = 0.2$ sample.

4. Conclusions

In summary, we have investigated high-temperature TE properties of a series of misfit-layered oxides $Ca_{2.9}Ln_{0.1}Co_4O_{9+\delta}$ (Ln = Dy, Ho, and Er) and $Ca_{3-x}Lu_xCo_4O_{9+\delta}$ with $x = 0$, 0.1, 0.2 and 0.3. These misfit-layered oxides are synthesized by conventional solid state reactions followed by hot-pressing. The results indicate that TE properties of $Ca_3Co_4O_{9+\delta}$ is effectively improved by late rare earths with smaller ionic radius, particularly that for the Lu-doped samples. The magnitude of ZT for the $Ca_{2.8}Lu_{0.2}Co_4O_{9+\delta}$ sample attains 0.36 at 1073 K, which seems to be the most significant improvement as compared to that for the Bi-, Sr-, Na-, Nd-, Gd-, Eu-, Y-, Gd/Y- and Yb-doped samples.

Acknowledgment

This work was supported by National Science Council of Taiwan, R.O.C. under the Grant Nos. NSC-95-2112-M-018-006-MY3 and NSC 98-2112-M-018-005-MY3. N.V. Nong would like to express thanks to the postdoctoral fellowship sponsored by National Science Council of Taiwan.

References

[1] D.M. Rowe, Renewable Energy 16 (1999) 1251–1256.
[2] I. Terasaki, Y. Sasago, K. Uchinokura, Phys. Rev. B 56 (1997) R12685–12687.
[3] M. Shikano, R. Funahashi, Appl. Phys. Lett. 82 (2003) 1851–1853.
[4] A.C. Masset, C. Michel, A. Maignan, M. Hervieu, O. Toulemende, S. Studer, et al., Phys. Rev. B 62 (2000) 166–175.
[5] T. Takeuchi, T. Kondo, K. Soda, U. Mizutani, R. Funahashi, M. Shikano, et al., J. Electron Spectrosc. Relat. Phenom. 137–140 (2004) 595–599.
[6] E. Guilmeau, R. Funahashi, M. Mikami, K. Chong, D. Chateigner, Appl. Phys. Lett. 85 (2004) 1490–1492.
[7] P. Limelette, V. Hardy, P. Auban-Senzier, D. Jérome, D. Flahaut, S. Hébert, R. Frésard, Ch. Simon, J. Noudem, A. Maignan, Phys. Rev. B 71 (2005) 233108–233111.
[8] J.G. Noudem, M. Prevel, A. Veres, D. Chateigner, J. Galy, J. Electroceram. 22 (2009) 91–97.
[9] X.-D. Zhou, L.R. Pederson, E. Thomsen, Z. Nie, G. Coffey, Electrochem. Solid-State Lett. 12 (2) (2009) F1–F3.
[10] D. Wang, L. Cheng, Q. Yao, J. Li, Solid State Commun. 129 (2004) 615–618.
[11] M. Prevel, E.S. Reddy, O. Perez, W. Kobayashi, I. Terasaki, C. Goupil, J.G. Noudem, Jpn. J. Appl. Phys. 46 (2007) 6533–6538.
[12] Y. Liu, Y. Lin, L. Jiang, C.-W. Nan, Z. Shen, J. Electroceram. 21 (2008) 748–751.
[13] Y. Wang, Y. Sui, J. Cheng, X. Wang, J. Miao, Z. Liu, et al., J. Alloys Compd. 448 (2008) 1–5.
[14] H.Q. Liu, Y. Song, S.N. Zhang, X.B. Zhao, F.P. Wang, J. Phys. Chem. Solids 70 (3-4) (2009) 600–603.
[15] H.Q. Liu, Y. Song, S.N. Zhang, X.B. Zhao, F.P. Wang, Curr. Appl. Phys. 9 (2009) 409–413.
[16] F.P. Zhang, Q.M. Lu, J.X. Zhang, Phys. B 404 (2009) 2142–2145.
[17] Y. Wang, Y. Sui, J. Cheng, X. Wang, W. Su, J. Alloys Compd. 477 (2009) 817–821.
[18] H.Q. Liu, Y. Song, S.N. Zhang, X.B. Zhao, F.P. Wang, J. Phys. Chem. Solids 70 (2009) 600–603.
[19] J. Xu, C. Wei, K. Jia, J. Alloys Compd. 500 (2010) 227–230.
[20] Y. Song, Q. Sun, L. Zhao, F. Wang, Key Eng. Mater. 434–435 (2010) 393–396.
[21] Y. Lu, Y. Song, J. Feng, F.P. Wang, Mater. Sci. Forum 650 (2010) 132–136.
[22] C.-J. Liu, L.-C. Huang, J.-S. Wang, Appl. Phys. Lett. 89 (2006) 204102–204104.
[23] J.L. Chen, Y.S. Liu, C.-J. Liu, L.-C. Huang, C.L. Dong, S.S. Chen, C.L. Chang, J. Phys. D: Appl. Phys. 42 (2009) 135418–135422.
[24] N.V. Nong, C.-J. Liu, M. Ohtaki, J. Alloys Compd. 491 (2010) 53–56.
[25] Y. Wang, Y. Sui, P. Ren, L. Wang, X. Wang, W. Su, H. Fan, Chem. Mater. 22 (2010) 1155–1163.

[26] W. Koshibae, K. Tsutsui, S. Maekawa, Phys. Rev. B 62 (2000) 6869–6872.
[27] C.-J. Liu, C.-Y. Liao, J.-S. Wang, P.K. Nayak, Z.-R. Lin, Appl. Phys. Lett. 91 (2007) 142509–142511.
[28] R. Asahi, J. Sugiyama, T. Tani, Phys. Rev. B 66 (2002) 155103–155119.
[29] C.-J. Liu, J.-L. Chen, L.-C. Huang, Z.-R. Lin, C.L. Chang, J. Appl. Phys. 102 (2007) 014908–014911.
[30] T.S. Chan, R.S. Liu, G.Y. Guo, S.F. Hu, J.G. Lin, J.M. Chen, J.P. Attfield, Chem. Mater. 15 (2003) 425–432.